Growth kinetics of CdSe nanoparticles in glass

M H Yükselici

Yıldız Technical University, Faculty of Science and Letters, Department of Physics,
34010 Davutpaşa, Topkapı/İstanbul, Turkey

Abstract
The growth of $CdS_{0.08}Se_{0.92}$ nanoparticles in glass is studied through the
analysis of optical absorption spectra with the help of a quantized-state effective-
mass model in which the conduction band effective mass is particle size
dependent. The glass includes nanoparticles with an initial average size of
$\sim$1.4 nm on cooling down to room temperature from the melt at $\sim$1000 °C.
Particles grow by diffusion of the reactants onto the surface of initially formed
nuclei upon heat treatment between 575 and 675 °C. Combined use of Arrhenius
plots and the model yields an activation energy of $\sim$500 kJ mol^{-1}.

1. Introduction

Size-selective optical absorption due to quantum confinement effects [1] provides a powerful
tool for investigating the nucleation and growth of semiconductor nanoparticles. Adjustment of
the growth kinetics parameters can be used to control the size, size distribution and number of
particles. Technological applications of nanoparticles require good control of these properties.
Solid-phase precipitation to produce nanoparticles in glass is a well-established straightforward
technique [2, 3]. The aim of the current research on nanoparticles is to establish a way to tune
for a given wavelength of light, and detailed studies on variations in optical properties with
the growth mechanisms of particles will help to improve our knowledge of the response of
nanoparticles/glass composites to light waves.

Fuyu and Parker [4] studied the growth of CdS_xSe_{1-x} particles in Zn-doped glass and
related the shift in the position of the first exciton peak to the heat treatment time to calculate
the activation energy for diffusion, 329 kJ mol^{-1}, from the Arrhenius plots. They did
not report the stoichiometry of the particles. This method was adapted by Sukumar and
Doremus [5] to calculate the activation energy 273 kJ mol^{-1} for the diffusive growth of CdS
nanoparticles in glass which contains Zn. They used the energies of the absorption edge
spectra rather than the energies of the positions of first exciton peaks, which were absent in
their optical absorption spectra. However, the growth of CdS particles in Zn-doped glass might
be dominated by homogeneous nucleation. Determination of the activation energy from the
shift of the absorption edge energy is expected to be problematic if the dominant mechanism
for the particle formation is homogeneous, in which case the rate of the shift of the exciton peak

position is much slower than that of the heterogeneously formed particles [6]. Banfi *et al* [7] used small-angle neutron scattering to predict an activation energy of $A/k_B = 30\,000$ K (250 kJ mol^{-1}) for the growth of CdS$_{1-x}$Se$_x$ particles with $x \approx 0.1$ in commercial Schott glass, which has a similar basic glass composition to the Schott glass used in this study. Liu and Risbud [8] analysed TEM measurements on CdSe particles in borosilicate glass and concluded that the early size distribution for a single sample was consistent with homogeneous nucleation theory. But they did not report optical absorption data, which can be used to distinguish between different mechanisms of particle formation from the evolution of the absorption spectrum over time [6]. Recent studies by Persans *et al* [9, 10] and Hayes *et al* [11] employed x-ray absorption, resonant Raman and optical absorption spectroscopies to study the growth of CdS nanoparticles in glass. They found that the formation of CdS particles is consistent with homogeneous nucleation followed by Lifshitz–Slyzov ripening. Hayes *et al* predicted a solubility activation energy of 0.55 eV (53 kJ mol^{-1}) for the limiting reactant from direct analysis of XAFS measurements of the Cd–S bond fraction.

In this work, optical absorption spectroscopy was employed to study the growth kinetics of CdS$_{0.08}$Se$_{0.92}$ nanoparticles in glass. The average radii of particles were determined by relating the energy of the position of the first exciton peak to the transition energy calculated using a simple quantized-state effective-mass model in which the conduction band effective mass is assumed to be particle size dependent. Precursors of a stable nucleus or nucleation centres form on cooling down the glass melt from $\sim$1000 °C to room temperature. Heat treatment at temperatures from 575 to 675 °C for various times leads to the diffusive growth of particles with average radii up to a few nanometres. The initial average radius of the particles before the heat treatment was determined and used in Arrhenius plots to obtain the activation energy for the rate-limiting reactant.

2. Sample preparation and experimental details

The samples were prepared from commercially available RG695 Schott filter glass. An as-received colour filter was sliced to dimensions of $10 \times 10 \times 1.5$ mm with a diamond saw. A number of these small samples were melted in an oven at about 1000 °C to dissolve the particles and then, by quickly removing the samples from the oven, quenched rapidly to room temperature to prevent reformation of the particles while cooling down. The samples turned from a dark-reddish colour to transparent. These colourless samples were placed in an isothermal heat treatment furnace at temperatures between 575 and 675 °C for various times. In all of the heat treatment processes, a platinum foil was used to isolate the samples from the ceramic boat so that the samples could shrink during quenching. The heat treated samples were ground to thicknesses of approximately 0.5 mm and then fully polished on both sides to give good quality surfaces. The typical basic glass composition of commercial Schott colour filters is given in [7] as 52% SiO$_2$, 20% K$_2$O, 20% ZnO, 5% B$_2$O$_3$. Wavelength-dispersive x-ray fluorescence measurements on one as-received glass before and after melting yielded similar molecular concentrations for the first three major components. The Schott glass filters with cut-off wavelengths in the visible range contain CdS$_x$Se$_{1-x}$ nanoparticles. Schott RG695 filter glass, which is the starting material for this study, is doped with CdS$_{0.08}$Se$_{0.92}$ semiconductor nanoparticles [7, 12].

All of the samples were characterized using optical absorption spectroscopy. The absorption edge spectra for the samples heat treated at 575 °C for up to 8 h and at 600 °C for up to 4.5 h have no peak. However, the absorption edge moves to lower energies with increasing heat treatment time for these samples. The straight-line portions of the absorption coefficient squared (α^2) against *energy* curves are extrapolated to obtain the absorption edge
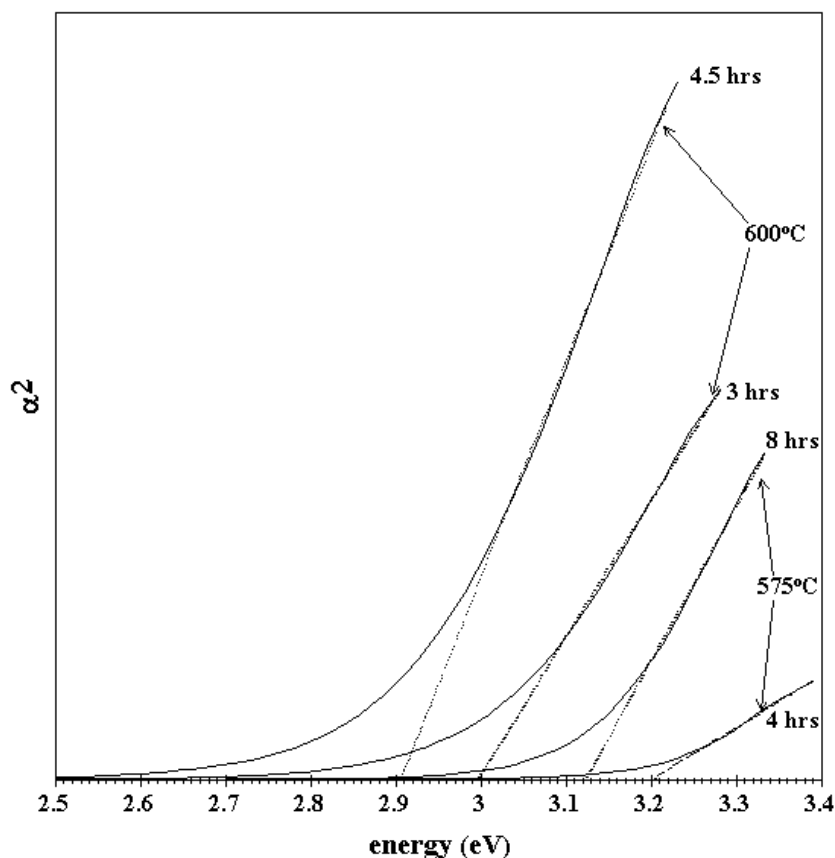
Figure 1. The square of the optical absorption coefficient (α^2) against energy, for $CdS_{0.08}Se_{0.92}$-doped glass samples heat treated at 575 and 600 °C. The straight-line portions are extrapolated to obtain the edge energies as intercepts at $\alpha^2 = 0$ (dotted lines).

energies as intercepts with the $\alpha^2 = 0$ line as shown in figure 1. The edge moves from ~3.2 to ~3.12 eV upon heat treatment at 575 °C for from 4 to 8 h. Treatment at 600 °C leads to a faster shift of the edge and moves the edge position after 4.5 h to down ~2.9 eV. Representative absorption edge spectra are shown in figure 2. The melted sample has very low absorption, increasing slightly up to ~3 cm^{-1} at ~3 eV. The absorption increases monotonically upon heat treatment at 625 °C for 1.5 h and a peak forms at ~2.5 eV after 2 h of heat treatment. The peak evolves over time to one characterized by clear structure at ~2.4 eV. Both the peak and the onset of the absorption move to lower energies simultaneously and the magnitude of the absorption increases as the heat treatment continues. The peak, while essentially keeping its shape, moves to ~2.1 eV upon heat treatment at 650 °C for 3 h. The peak becomes a shoulder and the absorption onset moves further to lower energies upon treatment at 675 °C for 2 h, approaching the absorption edge of the as-received glass.

3. Discussion

The formation of an absorption peak is associated with the absorption of light by semiconductor nanoparticles in glass. The observed shift of the peak to lower energies might be due mainly to quantum-size effects and/or changes in the composition of the particles. It has been previously
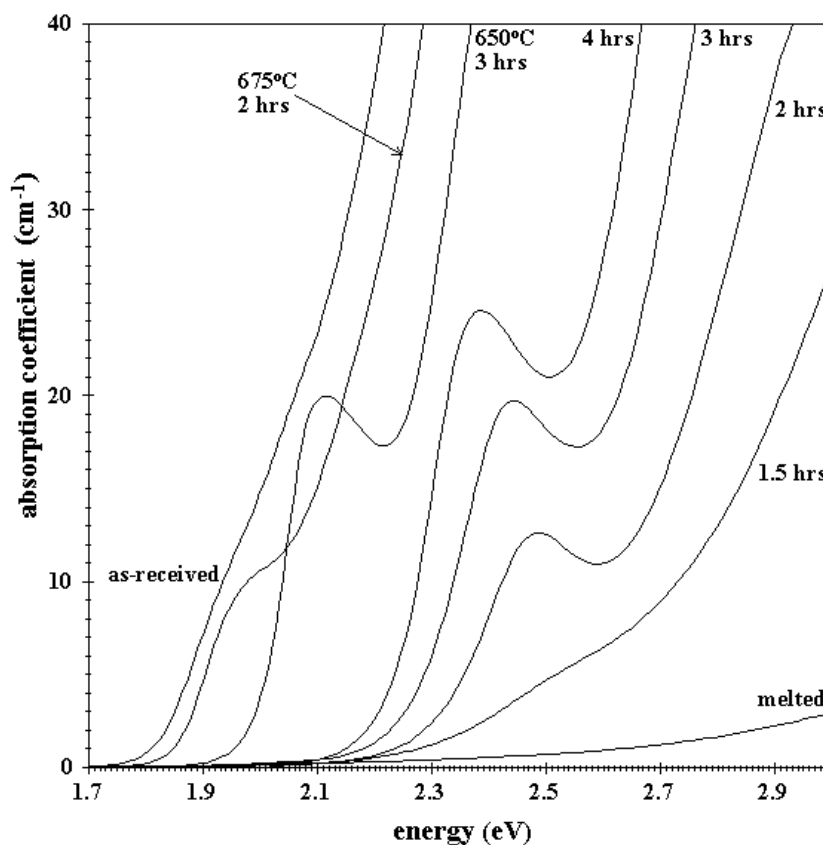
Figure 2. Optical absorption edge spectra for $CdS_{0.08}Se_{0.92}$-doped glass samples heat treated for various times at 625 °C unless otherwise stated. The spectrum marked 'melted' is the absorption spectrum for the as-received glass melted at ~1000 °C and quenched rapidly to room temperature.

reported that the S content of CdS_xSe_{1-x} particles decreases to some extent for longer heat treatment time. A 5% decrease in sulphur content over 68 h of heat treatment time at 625 °C was reported [6]. In contrast, higher heat treatment temperatures may result in a higher sulphur content incorporated into the particles over time: a 25 °C increase in heat treatment temperature can cause a 10% increase in the sulphur content of CdS_xSe_{1-x} nanoparticles [13]. That amount of decrease/increase in sulphur content in particles translates into a maximum change of ~20 meV in the band-gap energy of CdS_xSe_{1-x} nanoparticles for $x \leqslant 0.5$. However, this alone cannot account for the substantial shifts observed in figures 1 and 2 over comparably short periods of heat treatment time. That is why the shift in the absorption edge observed here is attributed mainly to the quantum-size effect and the peak as due to the production of an exciton in the lowest-energy bound state. As the particles grow over time, the first exciton peak moves to lower energies. The small blue-shift in energy above the bulk band gap of $CdS_{0.08}Se_{0.92}$, due to the quantum confinement effect, observed in the figure for the as-received sample, corresponds to an average nanoparticle radius of 4.6 nm [7]. The larger blue-shifts for other samples are indicative of nanoparticles with smaller average radius. Hence, the average radius of nanoparticles is less than the exciton Bohr radius ($a_B = 5.2$ nm for bulk CdSe) and therefore the confinement for electrons and holes in the CdSe particles is strong. In the strong-confinement regime, the position of the first exciton peak is given by [14]
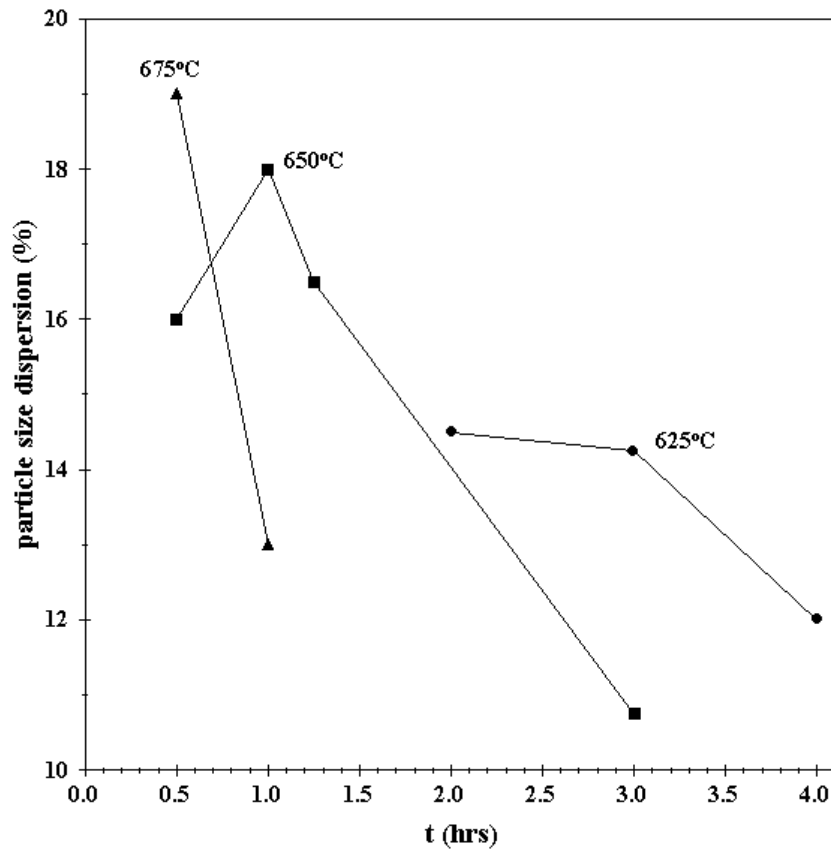
Figure 3. The width of the distribution in per cent of particle radius is plotted against heat treatment time for the CdS$_{0.08}$Se$_{0.92}$-doped glass samples treated at 625 ($\bullet$), 650 ($\blacksquare$) and 675 °C ($\blacktriangle$).

$$E_{n,l}(R) = E_g + \frac{A_{n,l}(R)}{R^2} \tag{1}$$

$$A_{n,l}(R) = \frac{\hbar}{2}\left[\frac{x^2_{n_e,l_e}}{m_e} + \frac{x^2_{n_h,l_h}}{m_h}\right] \tag{2}$$

where n, l are the electron or hole eigenstates 1s, 1p, 1d etc, $E_g = 1.83$ eV [15] is the band-gap energy of bulk CdS$_{0.08}$Se$_{0.92}$, R is the radius of the particle and x_{n_e,l_e} and x_{n_h,l_h} are the roots of the spherical Bessel function. Assuming that the conduction band effective mass is dependent on the radius of CdSe nanoparticles as $m_e = (0.13 + 1.4e^{-R})m_0$ due to nonparabolicity of the conduction band [16] in the strong-confinement regime and assuming a constant valence band effective mass of $m_h = 0.5m_0$ (m_0 is the electron rest mass), the average radius (R_{ave}) for the particles, the $A_{n,l}(R_{ave})$ coefficients and the particle size dispersion (Γ is the width of the distribution in per cent of particle radius) can be deduced by simulating the first exciton peak (1s state). A spin–orbit splitting energy of $E_{so} = 0.4$ eV and a natural line broadening of 60 meV were used in the model simulation. The details of the model calculation have been published elsewhere [6]. Each absorption edge spectrum was taken separately and the best-fit parameters for R_{ave}, $A_{1,0}$ (for the first exciton transition) and Γ were determined. In figure 3, particle size dispersion is plotted against heat treatment time. The squares of the average particle radii for each treatment temperature set are plotted against heat treatment time
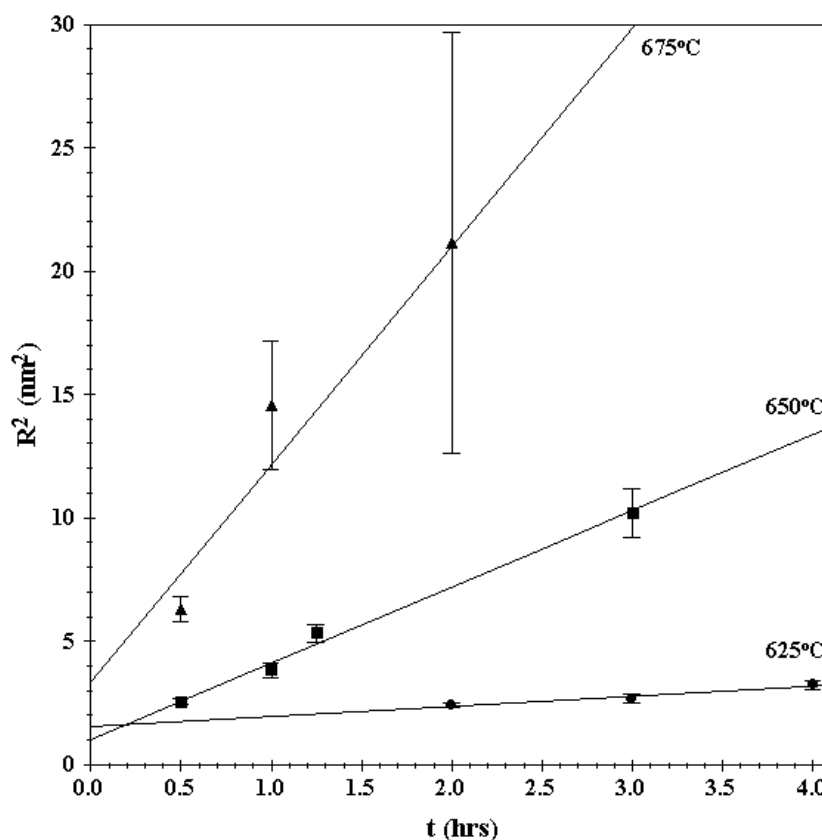
Figure 4. The square of the average particle radius (R_{ave}^2), deduced by simulating the first exciton peak (1s state), plotted against heat treatment time (t) for the CdS$_{0.08}$Se$_{0.92}$-doped glass samples treated at 625 (●), 650 (■) and 675 °C (▲). Solid lines show least-squares straight-line fits to the data.

in figure 4 and a least-squares straight-line fit to R_{ave}^2 plotted against heat treatment time is shown for each temperature. The result in figure 4 shows a well-defined linear relationship, which is an indication of diffusion-limited growth of particles. The evolution of the absorption edge spectra over time is consistent with heterogeneous nucleation of nanoparticles, followed by diffusive growth. The rate at which the absorption peak position moves to lower energies, i.e., $E/t = \sim 0.41$ eV h^{-1} at 625 °C, compares well with the previously reported rate of ~ 0.33 eV h^{-1} at 625 °C for the growth of CdS$_x$Se$_{1-x}$ particles with $x \approx 0.5$ in glass [6]. In diffusion-limited growth of the particles, all nuclei are assumed to be extrinsic and created at $t = 0$ prior to the heat treatment during the quenching of the melt to room temperature. As seen in figure 3, the narrowest particle size dispersion of $\sim 11\%$ is obtained for an average radius of ~ 3.2 nm at the end of heat treatment at 650 °C for 3 h. The maximum change in the particle size dispersion is only $\sim 8\%$ over the entire range of heat treatment time and temperature in this study. It is therefore reasonable to assume that the broadening of the size distribution around R_{ave} does not significantly affect the calculations developed below to extract the parameters for growth kinetics from the optical absorption data.

According to the diffusion-limited growth, for the case of quasi-static diffusion around a particle ($\nabla^2 C = 0$, $\partial C/\partial t \approx 0$), the average radius of the particles increases as [17]
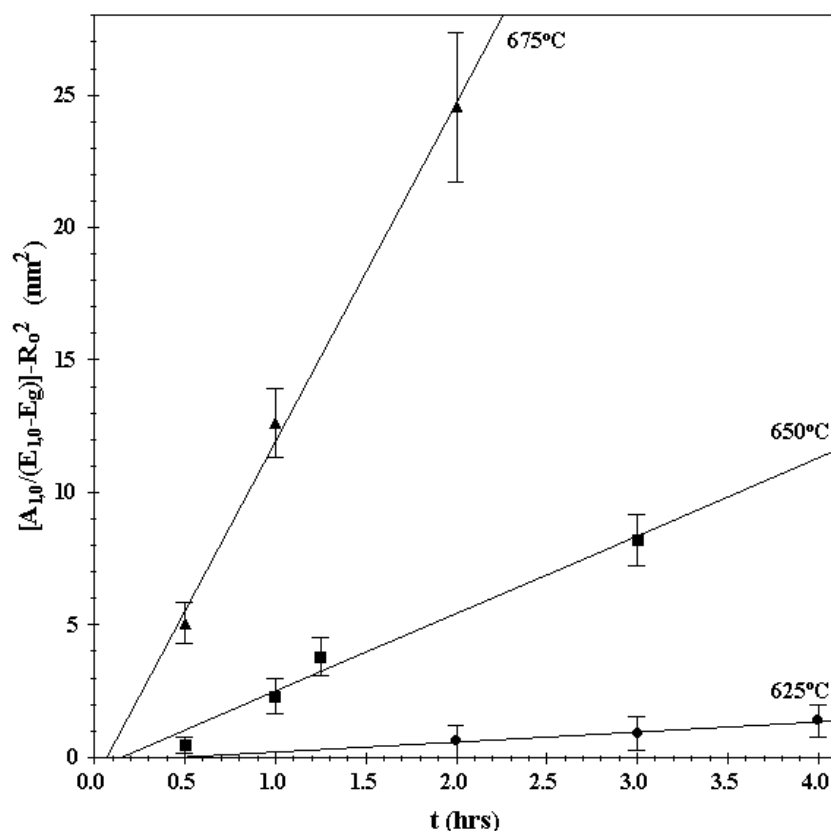
Figure 5. The expression $\{A_{1,0}(R_{ave})/[E_{1,0}(R_{ave}) - E_g]\} - R_0^2$ (see equations (4) and (6)), plotted against heat treatment time (t) for the $CdS_{0.08}Se_{0.92}$-doped glass samples treated at 625 (●), 650 (■) and 675 °C (▲). Solid lines show least-squares straight-line fits to the data.

$$R_{ave}^2 = R_0^2 + CDt \tag{3}$$

where D is a diffusion constant, t is the heat treatment time and $C = 2(C_\infty^\alpha - C_\beta^\alpha)/(C_\alpha^\beta - C_\beta^\alpha)$, where C_α^β is the concentration of the limiting reactant in the particles (β-phase), C_β^α is the concentration of the limiting reactant in the glass (α-phase), C_∞^α is the concentration of limiting reactant at the particle–glass interface (equilibrium concentration) and R_0 is the average radius of the particles at $t = 0$. The arithmetic mean of the extrapolated values of R_0^2 obtained for three temperature sets, as intercepts at $t = 0$ in figure 4, is ~ 2 nm^2; thus $R_0 = 1.4 \pm 0.2$ nm. This result indicates that the melted sample has crystallites with $R_0 = R(t = 0) \sim 1.4$ nm on cooling down to room temperature. The position of first exciton peak with $n = 1$, $l = 0$ is obtained by plugging equation (3) into (1):

$$E_{1,0}(R_{ave}) = E_g + \frac{A_{1,0}(R_{ave})}{R_0^2 + CDt}. \tag{4}$$

In figure 5, $\{A_{1,0}(R_{ave})/[E_{1,0}(R_{ave}) - E_g]\} - R_0^2$ is plotted against time for each heat treatment temperature. $E_{1,0}(R_{ave})$ is the energy of the first-exciton-peak centre determined by the position of the first minimum in the second derivative of the absorption spectrum. A least-squares fit to each temperature set shows a straight line, as expected from equation (4).
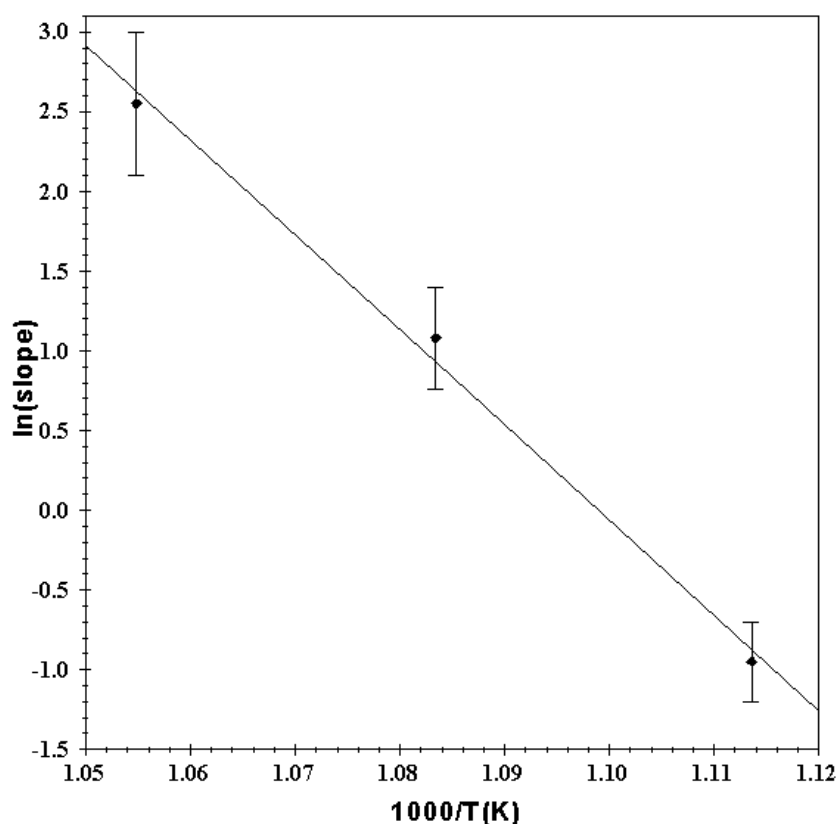
Figure 6. The natural logarithm of the slopes of the straight lines in figure 5, plotted against $1000/T$ (K) (T: heat treatment temperature). The solid line shows a least-squares straight-line fit to the data.

The diffusion coefficient at constant pressure is correlated with temperature through an Arrhenius relationship:

$$D = D_0 e^{-Q/RT} \tag{5}$$

where D_0 is a frequency factor, Q is the molar activation energy, R is the universal gas constant and T is the heat treatment temperature. Combining equations (4) and (5) yields

$$\ln \frac{\{A_{1,0}(R_{ave})/[E_{1,0}(R_{ave}) - E_g]\} - R_0^2}{t} = -\frac{Q(kJ)}{8.314} \frac{1000}{T\ (K)} + \ln(CD_0). \tag{6}$$

In figure 6, the natural logarithm of the slopes of the lines given in figure 5 is plotted against $1000/T$ (K). The activation energy of the diffusion is calculated as $Q = 500 \pm 80$ kJ mol^{-1} from the slope of the least-squares straight-line fit to the data in figure 6.

For a given concentration of basic glass, the activation energy varies depending on the rate-limiting reactant. The assumption adopted by early authors [4, 5] that the coefficients, $A_{1,0}(R_{ave})$, are constant leads to underestimation of the activation energy when the shift of the exciton peak position over time is used in Arrhenius plots. However, combined use of Arrhenius plots and the quantized-state effective-mass model, in which the conduction band effective mass is assumed to be increasing exponentially with decreasing particle radius, yields a comparatively high value of $\sim$500 kJ mol^{-1} of the activation energy for diffusive

growth of heterogeneously formed particles in $CdS_{0.08}Se_{0.92}$-doped glass. This result is double the previously reported one [7]—an independent determination of the activation energy of $250 \, kJ \, mol^{-1}$ for the growth of $CdS_{1-x}Se_x$ nanoparticles in Schott glass, which is expected to have a similar basic composition to the glass used in this study. Knowledge of the activation energy gives us control over when to cease the heat treatment in order to end up with a desired particle radius. The effect of the basic glass composition and the stoichiometry of the nanoparticle on the activation energy needs further research. The authors report two different values of activation energy for the early and late stages of the particle formation process. Therefore, it is also important to establish how the activation energy varies as a function of heat treatment time. Furthermore, it should be pointed out that the accuracy to which the value of the activation energy can be estimated with the method presented here is $\pm 80 \, kJ \, mol^{-1}$ as determined by error analysis. Supplementary measurements such as low-frequency Raman scattering or TEM analysis should be very useful for checking the sizes and size distribution determined. This will help improve the reliability of the method presented here, based on optical absorption spectroscopy.

4. Summary

As-received glass is quenched from the melt at $\sim 1000 \, ^\circ C$. Heat treatments at $575 \, ^\circ C$ for 8 h and at $600 \, ^\circ C$ for 3 h produce a pale yellow colour in the transmission, but no exciton peak or shoulder is observed in the optical absorption spectra. The effective-mass model taking into account the nonparabolicity of the conduction band predicts an average radius for $CdS_{0.08}Se_{0.92}$ particles of $\sim 1.4 \, nm$ on cooling down before heat treatment. Heat treatment at $625 \, ^\circ C$ for 2 h produces an orange colour in the transmission and an exciton peak in the absorption spectra. The peak evolves over time and becomes well defined at $\sim 2.35 \, eV$ after 4 h at $625 \, ^\circ C$ and at $\sim 2.1 \, eV$ after 3 h at $650 \, ^\circ C$. These clear peaks are indicative of a narrow distribution of particle radii with an average of $\sim 1.8 \, nm$ for $t = 4 \, h$ at $T = 625 \, ^\circ C$ and $\sim 3.2 \, nm$ for $t = 3 \, h$ at $T = 650 \, ^\circ C$. The size dispersion takes its narrowest value of 11% for a particle radius of $\sim 3.2 \, nm$ upon heat treatment at $650 \, ^\circ C$ for 3 h. The formation of a well-defined first exciton peak and its evolution over time are consistent with heterogeneous nucleation followed by diffusion-limited growth. Combined use of Arrhenius plots and the model yields an activation energy for the rate-limiting reactant of $\sim 500 \, kJ \, mol^{-1}$ over the temperature range from 625 to $675 \, ^\circ C$.

Acknowledgments

References

[1] Ekimov A I and Onushchenko A A 1982 *Sov. Phys.–Semicond.* **16** 775
[2] Borelli N F, Hall D, Holland H and Smith D 1987 *J. Appl. Phys.* **61** 5399
[3] Persans P D, Tu A, Wu Y-J and Lewis M 1988 *J. Opt. Soc. Am.* B **6** 818
[4] Fuyu Y and Parker J M 1988 *Mater. Lett.* **6** 233
[5] Sukumar V and Doremus R H 1993 *Phys. Status Solidi* b **179** 307

[6] Yükselici M H 2001 *J. Phys.: Condens. Matter* **13** 6123

[7] Banfi G P, Degiorgio V and Speit B 1993 *J. Appl. Phys.* **74** 6925

[8] Liu L C and Risbud S H 1990 *J. Appl. Phys.* **68** 28

[9] Persans P D, Lurio L B, Pant J, Yükselici H, Lian G and Hayes T M 2000 *J. Appl. Phys.* **87** 3850

[10] Persans P D, Lurio L B, Pant J, Lian G D and Hayes T M 2001 *Phys. Rev.* B **63** 115320

[11] Hayes T M, Lurio L B and Persans P D 2001 *J. Phys.: Condens. Matter* **13** 425

[12] Banfi G P, Degiorgio V and Ricard D 1998 *Adv. Phys.* **47** 447

[13] Roden W S O, Ironside C N and Torres C M S 1994 *Semicond. Sci. Technol.* **9** 1839

[14] Brus L E 1983 *J. Chem. Phys.* **79** 5566

[15] Madelung O (ed) 1982 *Semiconductors: Properties of II–VI Compounds* (Berlin: Springer)

[16] Nomura S and Kobayashi T 1991 *Solid State Commun.* **78** 677

[17] Glicksman M E 1994 *Diffusion in Solids* (Lecture Notes at RPI, Troy)